NASA Technical Memorandum 102834

A Brief Review of Some Mechanisms Causing Boundary Layer Transition at High Speeds

M. E. Tauber

June 1990

National Aeronautics and
Space Administration

NASA Technical Memorandum 102834

A Brief Review of Some Mechanisms Causing Boundary Layer Transition at High Speeds

M. E. Tauber, Ames Research Center, Moffett Field, California

June1990

National Aeronautics and
Space Administration

Ames Research Center
Moffett Field, California 94035-1000

SUMMARY

In high-speed flight, the state of the boundary layer can strongly influence the design of vehicles through its effect on skin friction drag and aerodynamic heating. The major mechanisms causing boundary layer transition on high-speed vehicles are briefly reviewed and some empirical relations from the unclassified literature are given for the transition Reynolds numbers.

INTRODUCTION

An understanding of the mechanisms which cause transition of the boundary layer from laminar to turbulent flow remains the most complex problem in fluid mechanics. At hypersonic speeds, turbulent boundary layer heating can be several times greater than laminar heating. Therefore, it is essential that some reliable means of predicting transition be available to avoid the penalties that result from overly conservative design. Because transition is influenced by many factors, the engineer must rely on empirical relations derived from test data. However, none of the ground test facilities can simulate most of the parameters of interest; in fact, the operating characteristics of many test facilities have been found to influence the data strongly. In the following sections, some examples of test data will be discussed and a few correlation charts and formulas will be presented.

NOMENCLATURE

k	surface roughness element height
L	total body length
M	Mach number
r	radius
Re	Reynolds number (boundary layer edge value, except in fig. 3)
T	temperature
w	crossflow velocity
x	distance along surface
δ	boundary layer velocity thickness
μ	coefficient of viscosity
ρ	density

Subscripts

btr or tr	beginning of transition
e	boundary layer edge value
n	vehicle nose
r	recovery or adiabatic wall value
sw	swallowing of high-entropy gas layer
w	wall condition
θ	boundary layer momentum thickness

MEASUREMENTS

It has long been known that among the important parameters influencing transition are the boundary layer edge Reynolds number and Mach number. The results of plotting measurements of the Reynolds number calculated at the beginning of transition against Mach number are shown in figure 1 for flow on cones. At first glance, figure 1 appears to be a shotgun pattern of data points with transition Reynolds numbers varying from about 1 million to 30 million. However, even within this jumble of data there are some definite trends. First, note that the flight data give the highest transition Reynolds numbers and the wind tunnel data give the lowest values. The ballistic range points fall, more or less, in the middle.

The occurence of early transition in many wind tunnels has been widely observed (refs. 1 and 2) and correlated by Dougherty and Fisher (ref. 2) with the intensity and, to some extent, the frequency of the free-stream disturbances in the facilities. The problems encountered in wind tunnel test measurements of transition have encouraged the use of ballistic ranges (refs. 3, 4, and 5). However, ballistic range experiments are affected by the small scale of the models which are, typically, on the order of a few centimeters in size. At that scale, microscopic surface irregularities and, possibly, dust particles suspended in the air can trigger transition. More recently, the development and use by Beckwith (ref. 6), of a low-disturbance, high Reynolds number, supersonic wind tunnel has yielded valuable data (refs. 7 and 8). For example, Chen et al. (ref. 8), measured similar transition Reynolds numbers at a Mach number of 3.5, on flat plates and slender cones with adiabatic walls. In high-noise wind tunnel tests at supersonic speeds, the transition Reynolds numbers on flat plates were only half as large as the values measured on cones (ref. 8), implying that the flat plate boundary layer was more sensitive to free-stream disturbances.

Many other phenomena can destabilize the laminar boundary layer. Among these are surface roughness, mass injection, positive pressure gradients, and wall heating or cooling (depending on the Mach number), as will be shown. In fact, any phenomenon which causes an inflection point to form in the boundary layer velocity profile is destabilizing (ref. 9). In contrast, boundary layer suction and negative pressure gradients have a stabilizing influence. While sucking hot air through the vehicle surface is highly impractical, it usually yields negative pressure gradients. One exception to the latter can occur when shock waves produced by different parts of the vehicle intersect. The resulting pressure rise can cause transition.

Although numerical calculations, using linear theory, have recently been made for simple shapes in high-speed flow (refs. 10 and 11), empirical correlations continue to be widely used, by necessity. Data have been collected and correlated with varying degrees of success for the phenomena causing boundary layer transition, and some examples will be discussed next.

EMPIRICAL CORRELATIONS

Despite the data scatter in figure 1, there is a discernible trend of increasing transition Reynolds number with rising Mach number. The same trend is shown more clearly in figure 2, which is based on references 12 and 13 for sharp cones tested primarily in wind tunnels. Note that the ballistic range measurements are, again, above most of the wind tunnel data. The high stability of the laminar boundary layer to disturbances at hypersonic edge Mach numbers has been observed by other researchers (ref. 14) and lends credence to the trend shown in figure 2. The data in figure 2 are for sharp cones. However, in practice

all bodies have finite amounts of nose bluntness. The nose bluntness introduces a second length scale, in addition to body size, into the transition problem.

Nose bluntness can have a very strong influence on transition as shown in figure 3 from reference 15. Note that the slopes of the lines change drastically at a value corresponding to about $r_n/x_{tr} = 10^{-2}$ for slender cones with half-angles of less than 10°. Therefore, the line labeled "small bluntness" is for very small amounts of nose blunting. The nose bluntness effect is caused by the action of the hot, high-entropy gas that has passed through the blunt portion of the bow shock. When the bluntness is "large," the shear layer produced by the entropy gradient in the inviscid part of the flow destabilizes the boundary layer. In contrast, if the nose blunting is very small, the thin high-temperature gas layer is "swallowed" much sooner (closer to the nose) by the boundary layer. As the gas flows downstream over the cone, the hot layer becomes progressively thinner and moves closer to the wall. This process increases the heating of the wall which can be stabilizing in hypersonic flow.

The effect of wall heating on slightly blunted slender cone transition was correlated in reference 5 using ballistic range data for cone half-angles from 3° to 9°. Subsequently, it was shown in reference 16 that flight measurements made on a 22° half-angle cone confirmed the slender cone ballistic range results (fig. 4) that wall heating stabilizes the hypersonic boundary layer, at least for surfaces that are well below the adiabatic wall temperature.

Unlike the hypersonic boundary layer, the thin subsonic and transonic one existing on the blunt noses of high-speed flight vehicles is easily tripped by surface roughness. The mechanism has been extensively studied and correlations have been published (refs. 17-19). Since strong pressure gradients exist on the blunt noses, the correlations use Reynolds numbers based on boundary layer momentum thickness rather than the body lengths used for sharp cones and flat plates. A formula suggested by Laderman (ref. 18) is

$$\mathrm{Re}_{\theta_{tr}} = 215 \Big/ \left(\frac{k}{\theta}\frac{T_e}{T_w}\right)^{0.7} \tag{1}$$

where k/θ is the ratio of roughness element height to local momentum thickness. (Charts of momentum thickness in high-speed flight for bodies with various amounts of nose bluntness can be found in ref. 20.) Another correlation for surface-roughness-induced transition is presented by Amirkabirian et al. (ref. 21) for the Shuttle orbiter and is shown in figure 5. Although the Shuttle tiles' surfaces are very smooth, the "roughness" results from misaligned tiles and the gaps that can form between tiles. Again, the majority of the flight data points are well above the shaded band which is based on wind tunnel tests.

It is valid to use local Reynolds numbers that are based on momentum thickness in preferrence to body length to correlate transition measurements on surfaces with pressure gradients. An approximate correlation for supersonic, or hypersonic, boundary layer edge velocities is (ref. 21)

$$\mathrm{Re}_\theta/\mathrm{M}_e = \text{const}. \tag{2}$$

where the constant varies from 150 to 350 depending on the ratio of roughness height to momentum thickness, etc. Another rationale for equation 2 is that it appears to yield a better correlation, with less data scatter, than using length Reynolds number, Re_x. However, the above reasoning is faulty. For example, for the incompressible flow over a flat plate $\mathrm{Re}_\theta \sim \mathrm{Re}_x^{0.5}$, or $x \sim \theta^2$. Therefore, using either Re_θ or Re_x will result in approximately the same uncertainty in the location of the beginning of transition on a flat plate.

One source of surface roughness is ablation of the heat shield. Another byproduct of ablation which destabilizes the boundary layer is gaseous mass addition. The effect of mass addition by transpiration of gases through a porous surface on transition on blunt bodies is presented in reference 22.

Some transition data are also available for configurations of practical interest, such as blunted cones at angle of attack (ref. 23), and swept-wing leading edges (ref. 24) where crossflow occurs. Crossflow can trigger transition by causing the formation of an inflection point in the inviscid shock layer velocity profile. A crossflow, boundary layer edge Reynolds number, which is approximately independent of Mach number, can be used to correlate transition, when written as

$$\mathrm{Re} = \frac{\rho_e w_e \delta}{\mu_e} \approx 350 \tag{3}$$

In equation 3, w_e is the maximum crossflow velocity and δ is the boundary layer velocity thickness. The remaining terms in the equation are evaluated at the boundary layer edge. The crossflow velocity, w, must be computed using three-dimensional flow field codes, or it can be measured, although with difficulty. The constant of 350 is based on transonic and supersonic flight test data (refs. 25-27) and is supported by measurements made in the quiet supersonic wind tunnel (ref. 7) at Mach 3.5. In contrast, tests conducted in standard ("noisy") wind tunnels yielded values of 175 to 200 for the crossflow transition Reynolds number. These low values indicate that test-facility-generated disturbances can also cause early crossflow-induced transition.

CONCLUDING REMARKS

The major mechanisms causing boundary layer transition are briefly discussed and some empirical relations are given for the transition Reynolds numbers. The effects on transition of local Mach number, nose bluntness, wall temperature, surface roughness, mass injection, and crossflow are covered. It is shown that transition is significantly delayed as local Mach number increases. However, despite the high transition Reynolds numbers which may occur at hypersonic speeds, many large vehicles will still experience turbulent boundary layers over much of their surfaces.

REFERENCES

1. Owen, F. K.; and Horstman, C. C.: Hypersonic Transitional Boundary Layers. AIAA Journal, vol. 10, no. 6, June 1972.

2. Dougherty, N. S., Jr.; and Fisher, D. F.: Boundary Layer Transition on a 10-Degree Cone: Wind Tunnel/Flight Data Correlation. AIAA Paper 80-0154, Jan. 1980.

3. Wilkins, M. E.; and Tauber, M. E.: Boundary-Layer Transition on Ablating Cones at Speeds up to 7 km/sec. AIAA Journal, vol. 4, no. 8, Aug. 1966.

4. Potter, J. L.: Boundary-Layer Transition on Supersonic Cones in an Aeroballistic Range. AIAA Journal, vol. 13, no. 3, March 1975.

5. Sheetz, N. W.: Free-Flight Boundary Layer Transition Investigations at Hypersonic Speeds. AIAA Paper 65-127, Jan. 1965.

6. Beckwith, I. E.: Development of a High Reynolds Number Quiet Tunnel for Transition Research. AIAA Journal, vol. 13, no. 3, Mar. 1975.

7. Beckwith, I. E.; Creel, T. R., Jr.; Chen, F. J.; and Kendall, J. M.: Free-Stream Noise and Transition Measurements on a Cone in a Mach 3.5 Pilot Quiet Tunnel. NASA TP-2180, Sept. 1983.

8. Chen, F. J.; Malik, M. R.; and Beckwith, I. E.: Comparison of Boundary Layer Transition on a Cone and Flat Plate at Mach 3.5. AIAA Paper 88-0411, Jan. 1988.

9. Schlichting, H.: Boundary Layer Theory. 7th Edition, McGraw-Hill, New York, NY, 1979.

10. Malik, M. R.; Spall, R. E.; and Chang, C. L.: Effect of Nose Bluntness on Boundary Layer Stability and Transition. AIAA Paper 90-0112, Jan. 1990.

11. Malik, M. R.: Prediction and Control of Transition in Supersonic and Hypersonic Boundary Layers. AIAA Journal, vol. 27, no. 11, 1989, pp. 1487-1493.

12. Donaldson, C. du P.; Sullivan, R. D.; and Yates, J. E.: An Attempt to Construct an Analytical Model of the Start of Compressible Transition. Flight Dynamics Lab., Wright-Patterson Air Force Base, Dayton, OH, AFFDL-TR-70-153, Jan. 1971.

13. Softley, E. J.; Graber, B. C.; and Zempel, R. E.: Experimental Observation of Transition of the Hypersonic Boundary Layer. AIAA Journal, vol. 7, no. 2, Feb. 1969.

14. Whitfield, J. D.; and Iannuzzi, F. A: Experiments on Roughness Effects on Cone Boundary-Layer Transition Up to Mach 16. AIAA Journal, vol. 7, no. 3, Mar. 1969.

15. Softley, E. J.: Transition of the Hypersonic Boundary Layer on a Cone: Part II – Experiments at M = 10 and More on Blunt Cone Transition. General Electric Space Sciences Lab., Missile and Space Division, Valley Forge, PA, Rept. R68SD14, Oct. 1968.

16. Sherman, M. M.; and Nakamura, T.: Flight Test Measurements of Boundary-Layer Transition on a Nonablating 22° Cone. Journal of Spacecraft and Rockets, vol. 7, Feb. 1970, pp. 137-142.

17. Swigart, R. J.: Roughness-Induced Boundary-Layer Transition on Blunt Bodies. AIAA Journal, vol. 10, no. 10, Oct. 1972.

18. Laderman, A. J.: Effect of Surface Roughness on Blunt Body Boundary-Layer Transition. Journal of Spacecraft and Rockets, vol. 14, no. 4, Apr. 1977.

19. Batt, R. G.; and Legner, H. H.: A Review of Roughness Induced Nosetip Transition. AIAA Paper 81-1223, June 1981.

20. Detra, R. W.; and Hidalgo, H.: Generalized Heat Transfer Formulas and Graphs for Nose Cone Re-Entry Into the Atmosphere. ARS Journal, Mar. 1961.

21. Amirkabirian, I.; Bertin, J. J.; Cline, D. D.; and Goodrich, W. D.: Effects of Disturbances on Shuttle Transition Measurements – Wind Tunnel and Flight. AIAA Paper 85-0902, Jan. 1985.

22. Kaattari, G. E.: Effects of Mass Addition on Blunt-Body Boundary-Layer Transition and Heat Transfer. NASA TP-1139, 1978.

23. Stetson, K. F.: Effect of Bluntness and Angle of Attack on Boundary Layer Transition on Cones and Biconic Configurations. AIAA Paper 79-0269, Jan. 1979.

24. Creel, T. R., Jr.; Beckwith, I. E.; and Chen, F. J.: Transition on Swept Leading Edges at Mach 3.5. AIAA Journal of Aircraft, vol. 24, no. 10, Oct. 1987.

25. Collier, F. S., Jr.; and Johnson, J. B.: Supersonic Boundary Layer Transition on the LaRC F-106 and the DFRF F-15 Aircraft. Part I: Transition Measurements and Stability Analysis. NASA CP-2487, Part 3, pp. 998-1014, 1987.

26. Maddalon, D. V.; Collier, F. S., Jr.; Montoya, L. C.; and Land, C. K.: Transition Flight Experiments on a Swept Wing with Suction. AIAA Paper 89-1893, 1989.

27. Collier, F. S., Jr.; Bartlett, D. W.; and Tat, V. V.: Correlation of Boundary Layer Stability Analysis with Flight Transition Data. IUTAM 3rd International Symposium on Laminar-Turbulent Transition, Toulouse, France, Sept. 11-15, 1989.

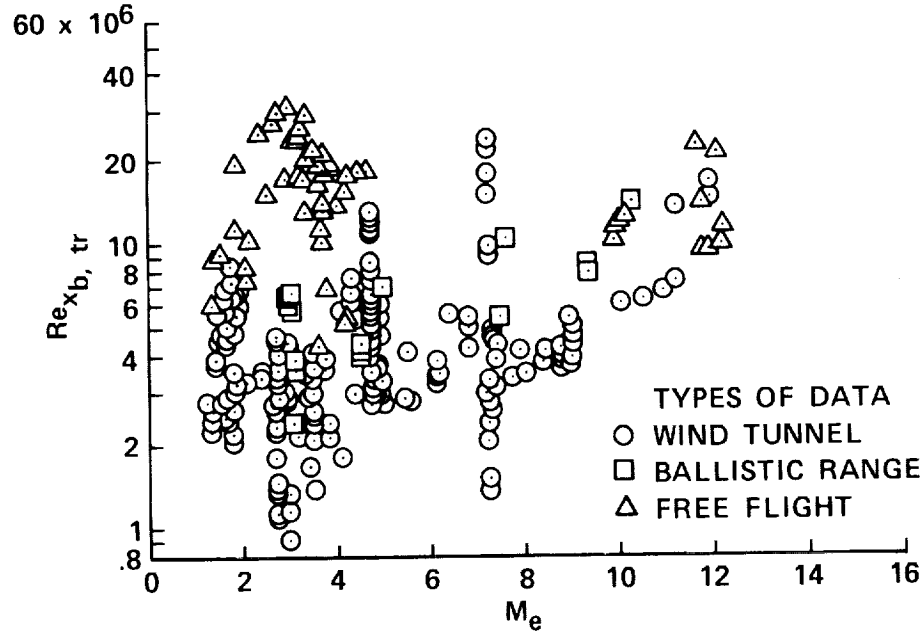

Figure 1. Typical transition data—cones.

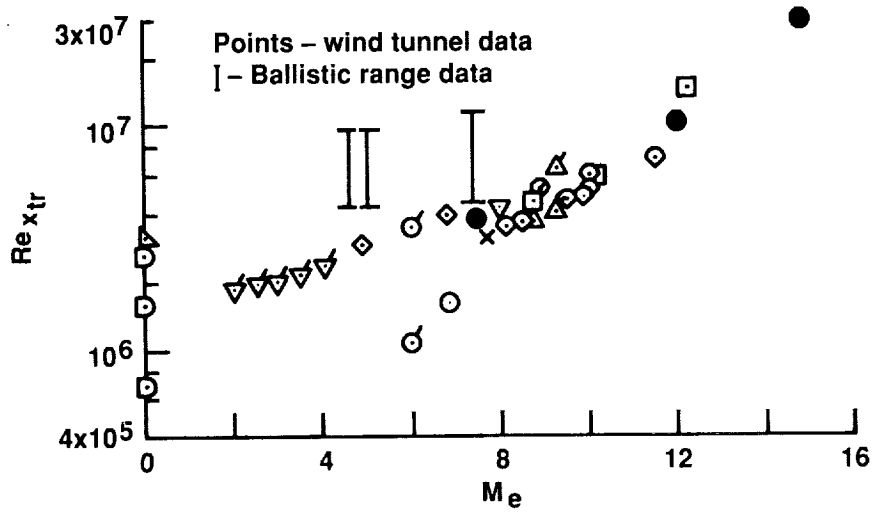

Figure 2. Sharp-cone transition local Reynolds number as a function of local Mach.

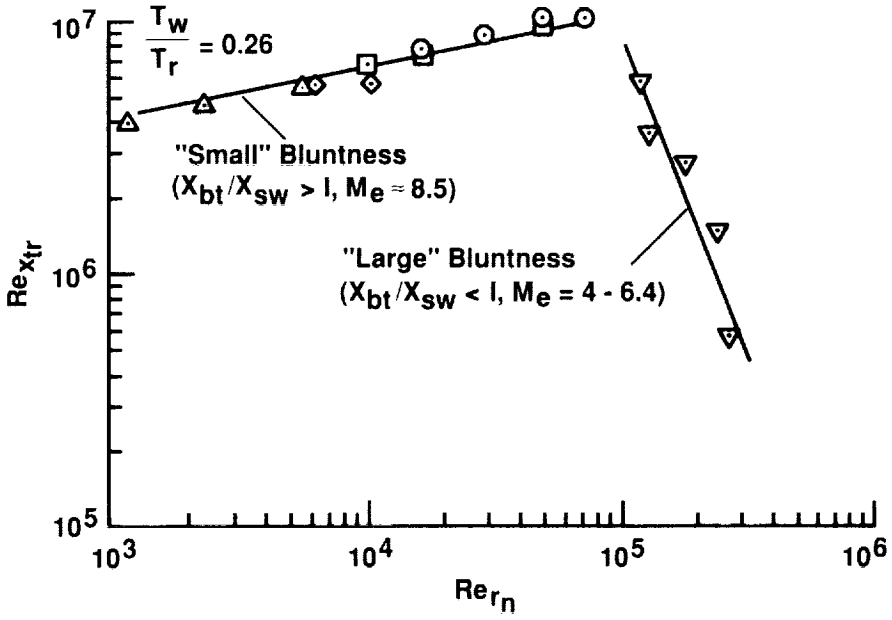

Figure 3. Transition Reynolds number (free-stream) on blunt cones in hypersonic flow.

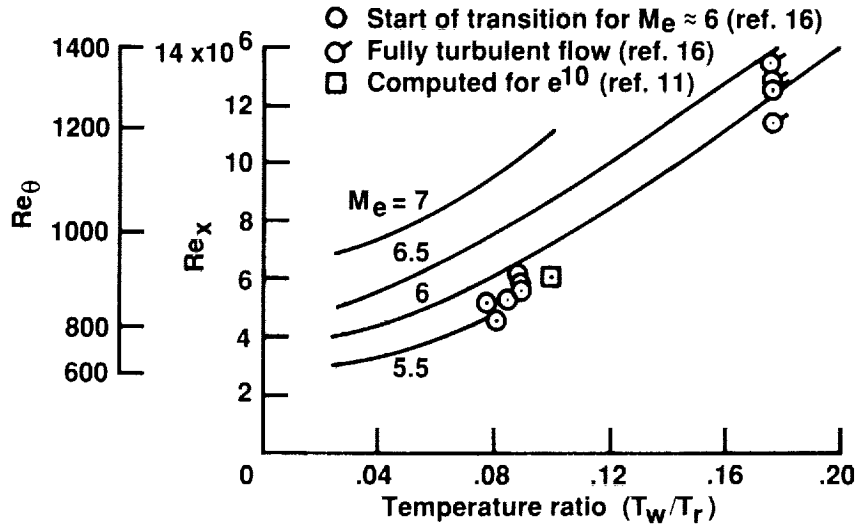

Figure 4. Effect of wall temperature on transition at hypersonic speeds.

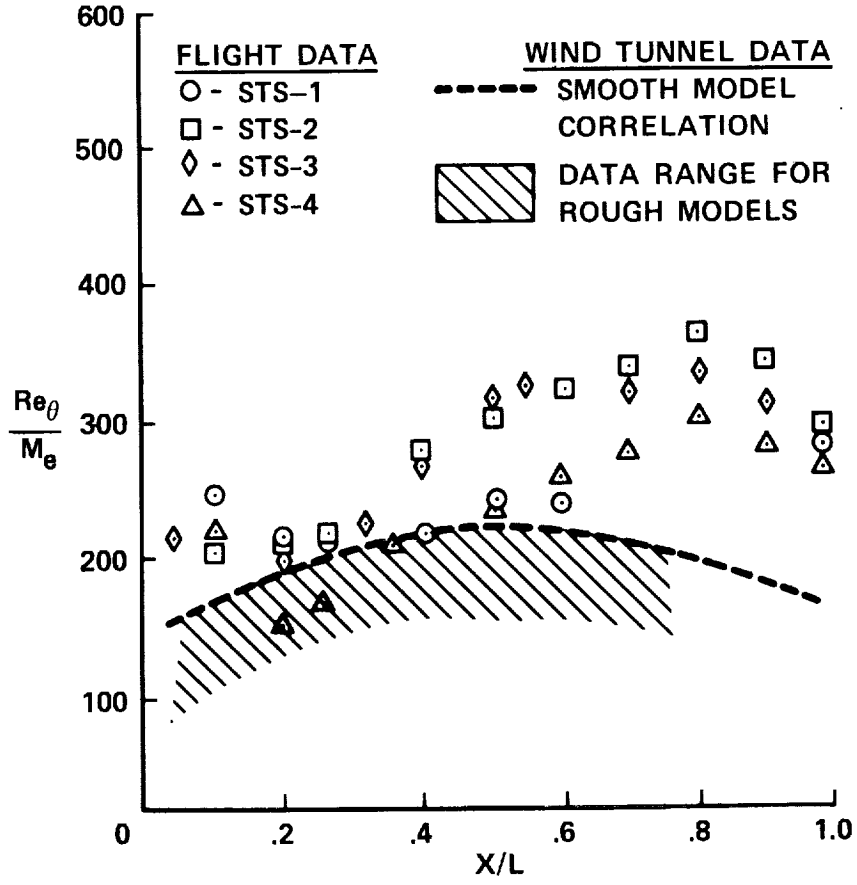

Figure 5. Shuttle orbiter flight values of the transition parameters (from ref. 21; reprinted with permission of the American Institute of Aeronautics and Astronautics).

NASA
National Aeronautics and Space Administration

Report Documentation Page

1. Report No.	2. Government Accession No.	3. Recipient's Catalog No.
NASA TM-102834		

4. Title and Subtitle

A Brief Review of Some Mechanisms Causing Boundary Layer Transition at High Speeds

5. Report Date

June 1990

6. Performing Organization Code

7. Author(s)

M. E. Tauber

8. Performing Organization Report No.

A-90186

10. Work Unit No.

591-42-11

9. Performing Organization Name and Address

Ames Research Center
Moffett Field, CA 94035-1000

11. Contract or Grant No.

13. Type of Report and Period Covered

Technical Memorandum

12. Sponsoring Agency Name and Address

National Aeronautics and Space Administration
Washington, DC 20546-0001

14. Sponsoring Agency Code

15. Supplementary Notes

Point of Contact: M. E. Tauber, Ames Research Center, MS 230-2
Moffett Field, CA 94035-1000
(415) 604-6086 or FTS 464-6086

16. Abstract

In high-speed flight, the state of the boundary layer can strongly influence the design of vehicles through its effect on skin friction drag and aerodynamic heating. The major mechanisms causing boundary layer transition on high-speed vehicles are briefly reviewed and some empirical relations from the unclassified literature are given for the transition Reynolds numbers.

17. Key Words (Suggested by Author(s))	18. Distribution Statement
Boundary layer transition Hypersonic	Unclassified-Unlimited Subject Category - 02

19. Security Classif. (of this report)	20. Security Classif. (of this page)	21. No. of Pages	22. Price
Unclassified	Unclassified	12	A02